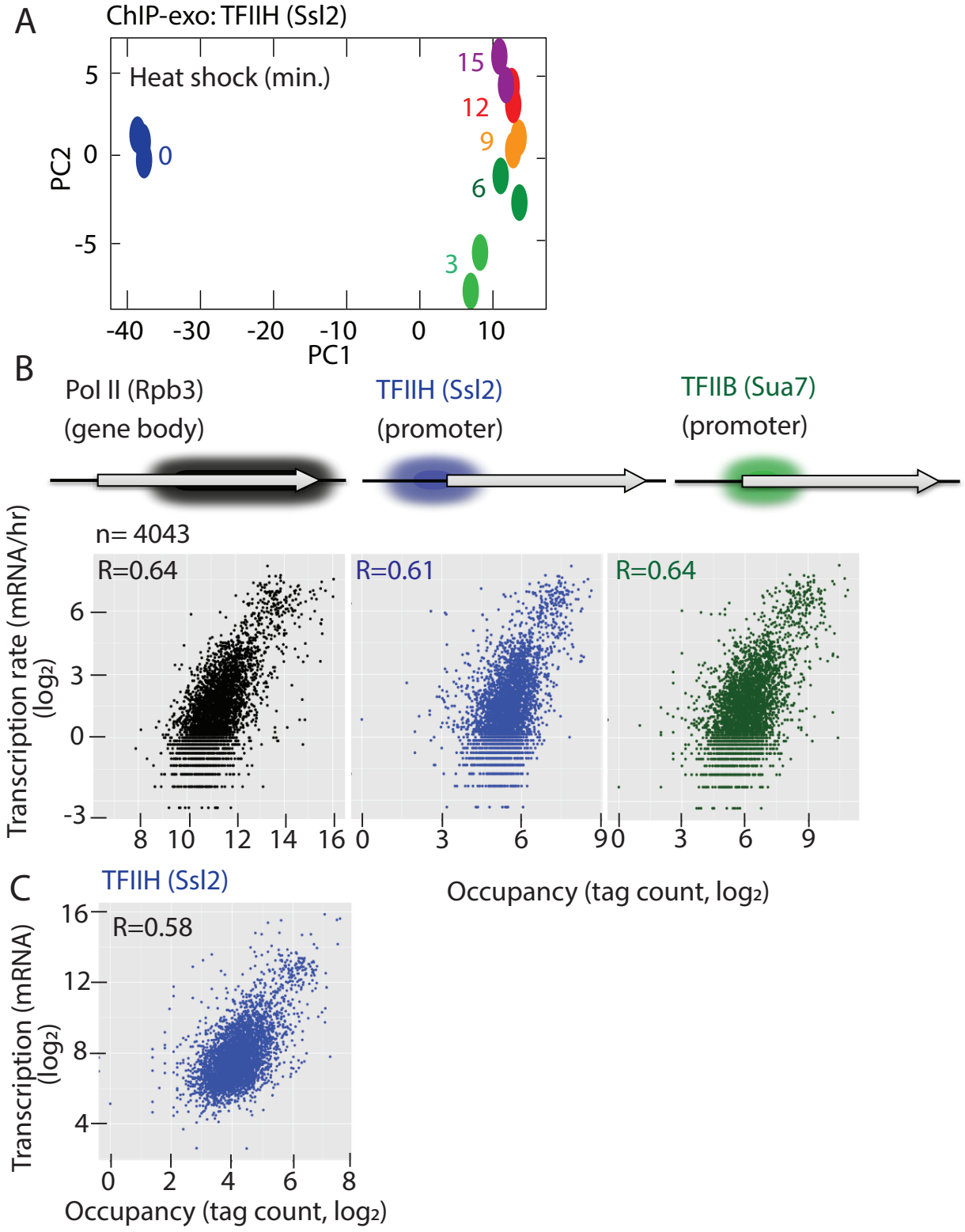

Supplemental Figure S1. ChIP-exo data consistency. (*A*) Principal component analysis (PCA) of TFIIH (Ssl2) occupancy comparing two biological replicates (same color ovals), each at various time points of heat shock. (*B*) Scatter plots representing Pearson correlation between transcription rate (mRNA/hr) (Holstege et al. 1998) and ChIP-exo occupancy of Pol II (black) in gene bodies (from TSS+100 bp to TES), TFIIH (Ssl2) (blue), and TFIIB (Sua7) (green) in promoters. Ssl2 and Sua7 were measured in regions spanning 100 bp upstream and downstream of the TSS. R-values from correlation are presented in the *left* corner. (*C*) Pearson correlation of TFIIH (Ssl2) occupancy and mRNA levels, using RNA-seq data from (Yassour et al. 2009).

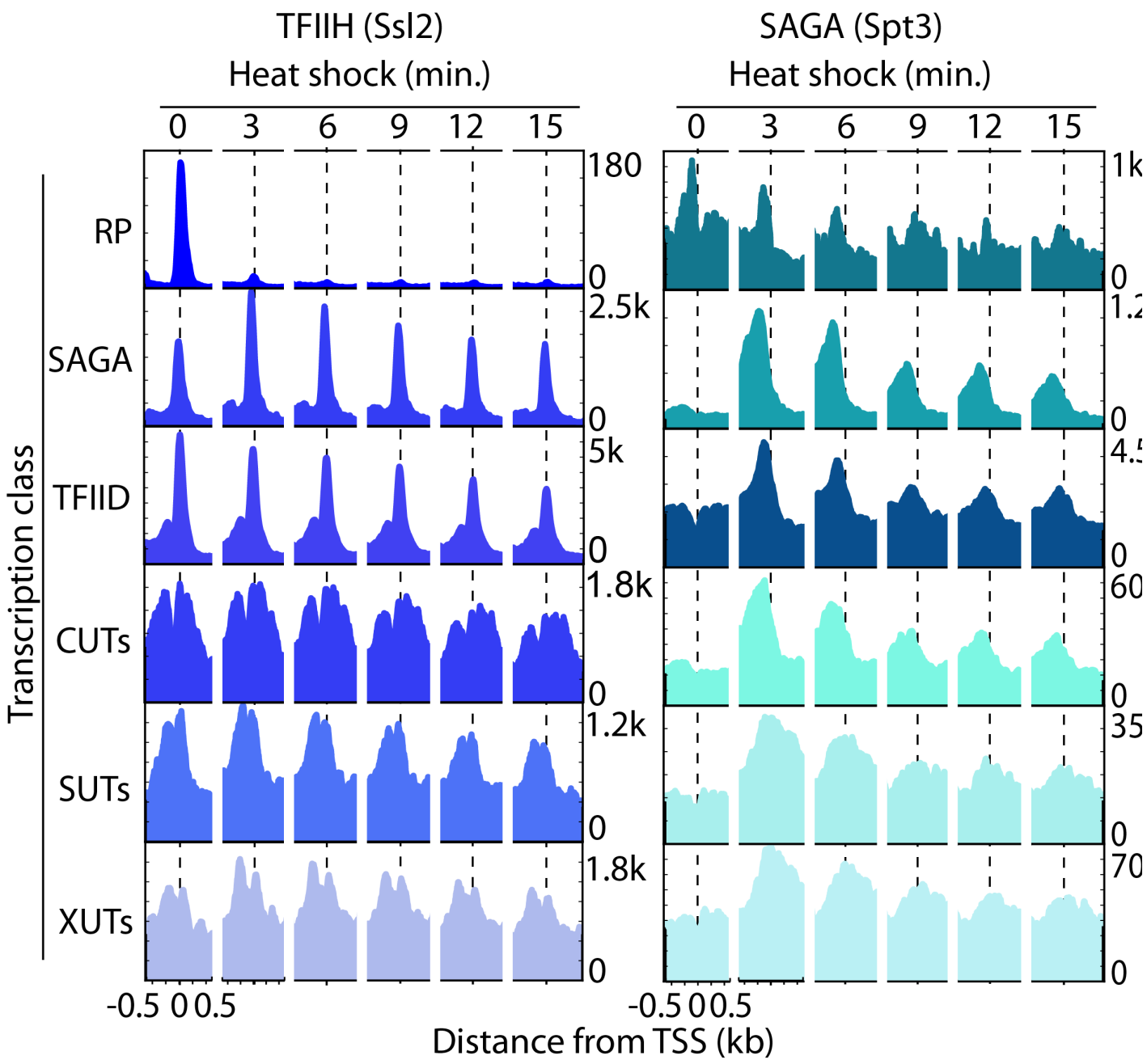

Supplemental Figure S2. Genome-wide dynamics of TFIIH and SAGA occupancy at coding and noncoding RNA classes. TFIIH (Ssl2) and SAGA (Spt3) averaged occupancy (normalized shifted tags) were distributed with respect to TSS, and organized into classes.

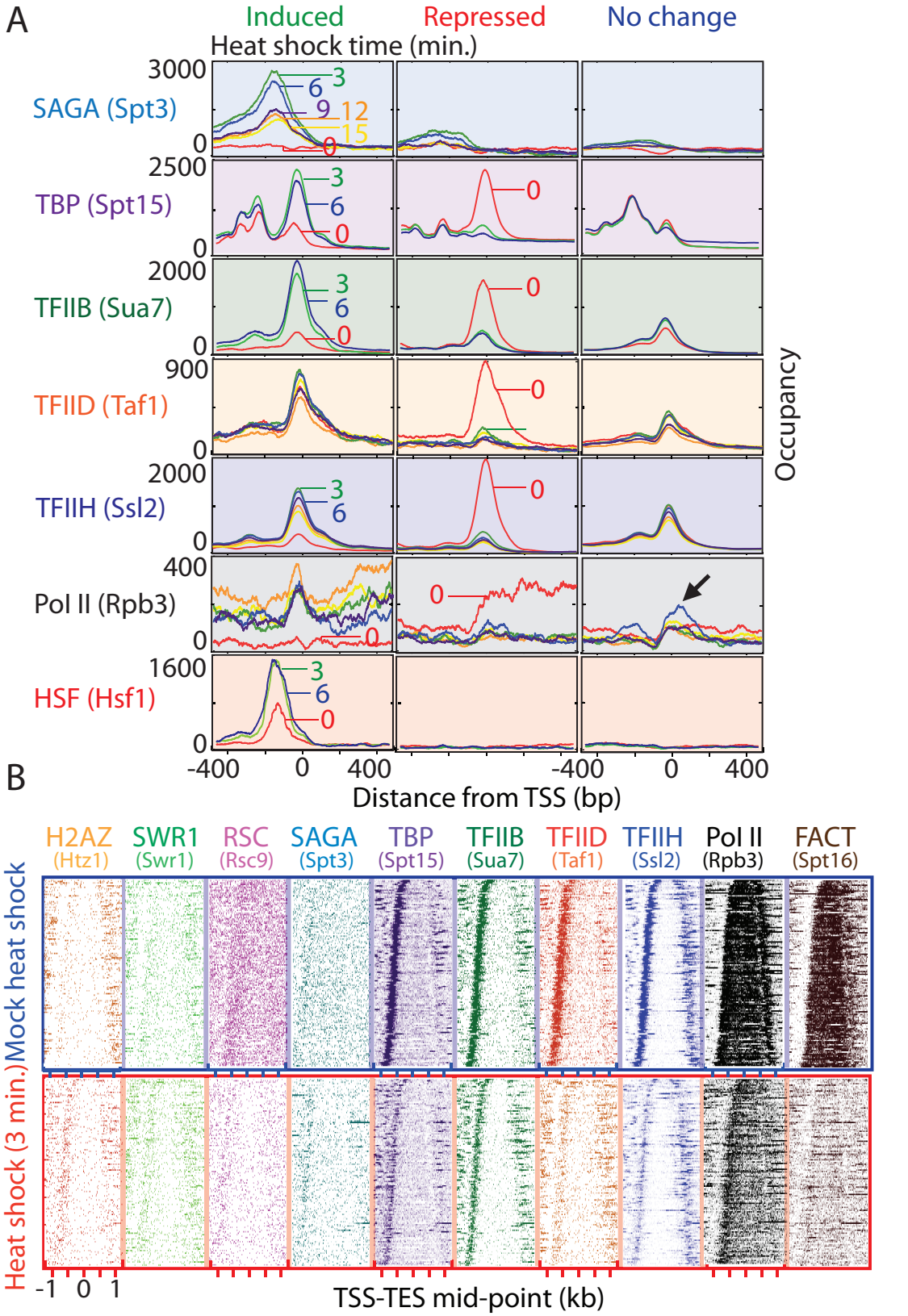

Supplemental Figure S3. Genome-wide dynamics of factor occupancy at induced and repressed coding genes. (*A*) Averaged normalized occupancy for coding genes that were either induced, repressed, or had no change in TFIIH (Ssl2) occupancy upon the indicated heat shock time points. The arrow points to an example of Pol II enrichment upon heat shock, without gene expression change. (*B*) Y-axis enlargement of RP genes from Fig. 2. The Spt3 mock heat shock dataset has a somewhat higher RP occupancy in other Spt3 replicates and other SAGA subunits than shown here.

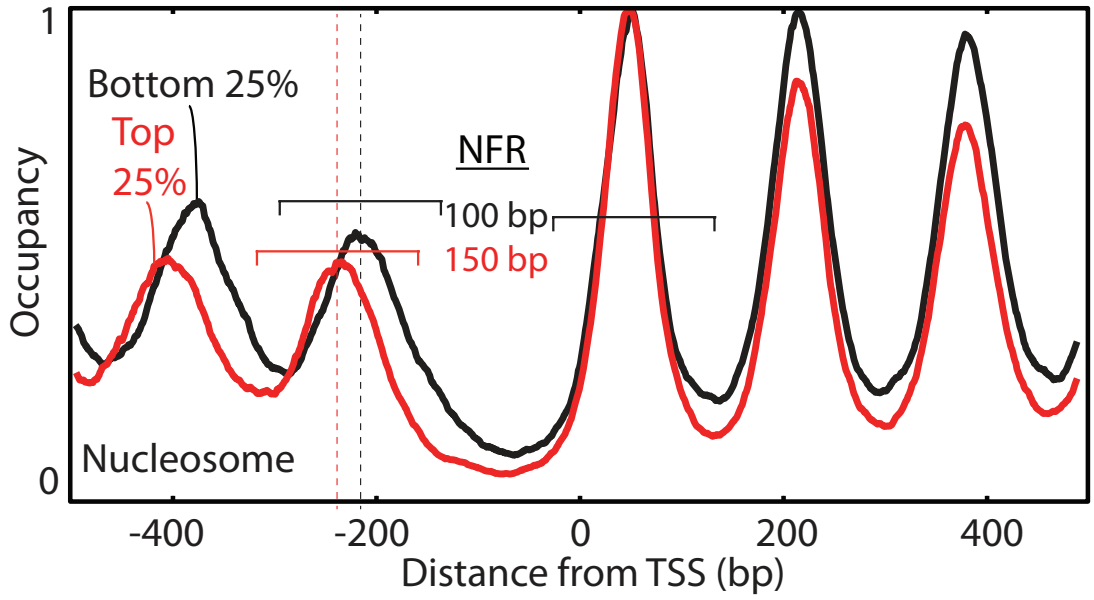

Supplemental Figure S4. Composite plot of nonheat shock nucleosome occupancy from the top and bottom 25% of GTF-occupied genes (TFIID-dominated class in Fig. 2., n = 4,260), sorted by TFIIH occupancy in the region from 100 bp upstream to 100 bp downstream of the TSS. Brackets denote the 147 bp of nucleosome-bound DNA.

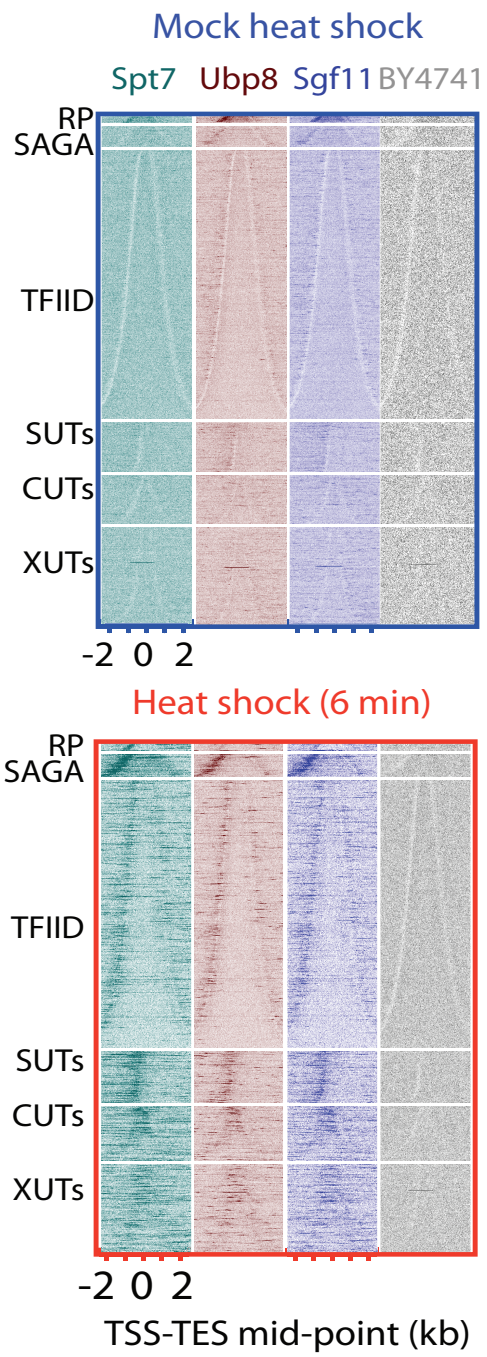

Supplemental Figure S5. Genome-wide distribution of other SAGA subunits that are unique to SAGA, before and after heat shock. See Figure 2 for figure description.

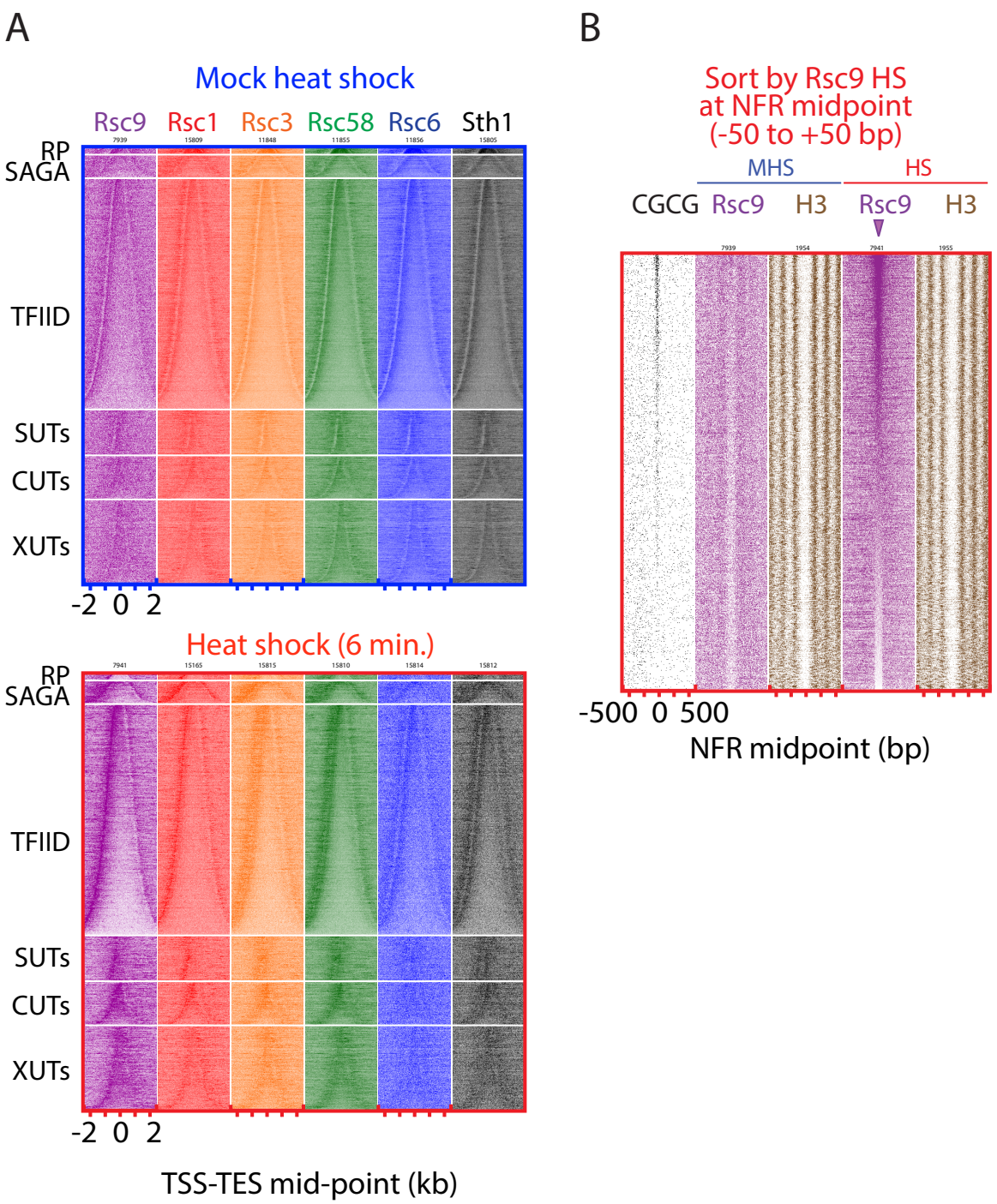

Supplemental Figure S6. RSC relocates to the Rsc3 motif upon heat shock. (*A*) Genome-wide distribution of RSC subunits at all coding genes, before and after heat shock. See Figure 2 for figure description. (*B*) All coding genes sorted by Rsc9 occupancy in heat shock (purple triangle). Upon heat shock, Rsc9 relocates to NFRs containing the Rsc3 motif (CGCG) (Badis et al. 2008); whereas nucleosome positions remain mostly unchanged. Panels are linked.

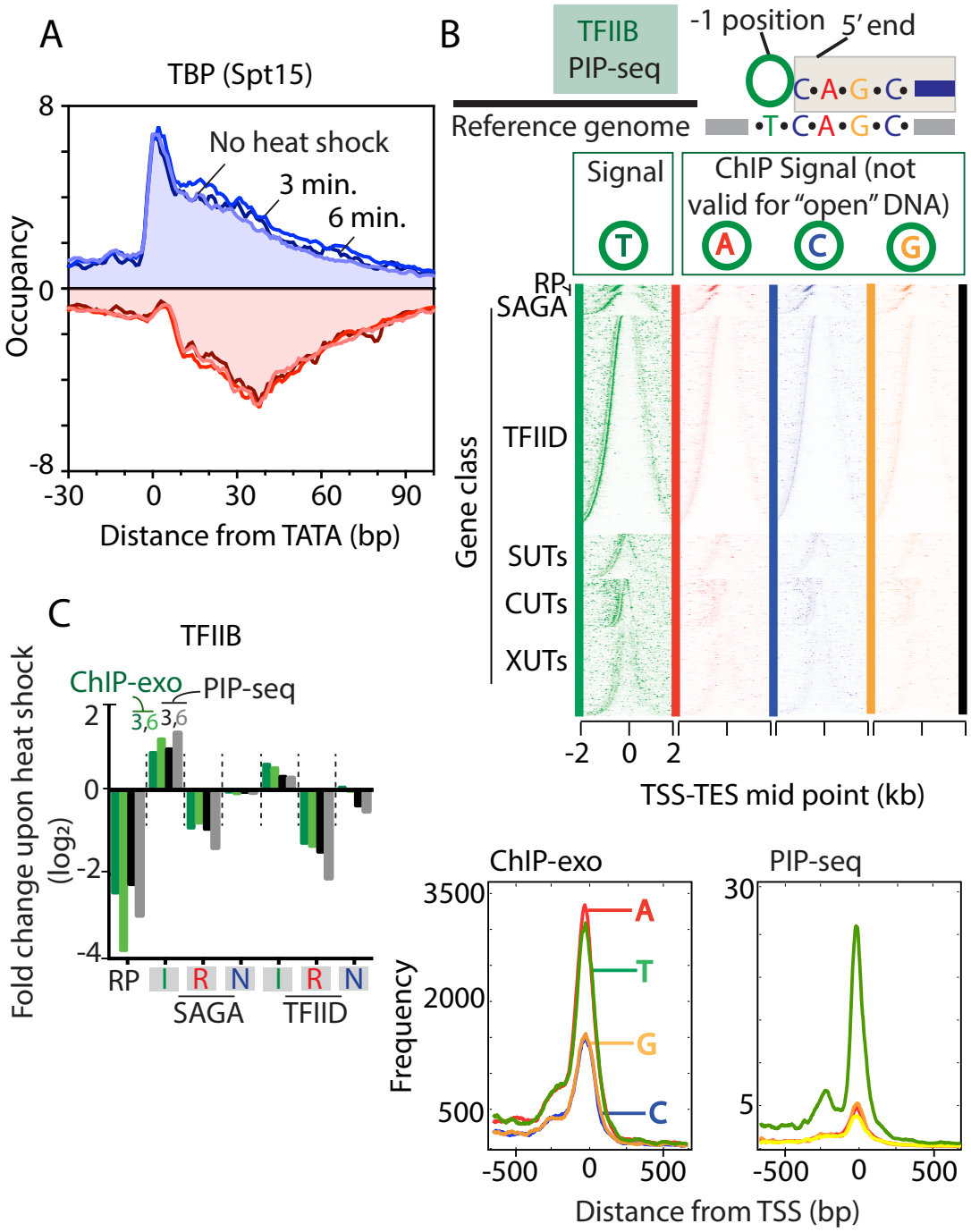

Supplemental Figure S7. (*A*) Strand separated tags from TBP (Spt15) sense-strand (light blue) and antisense-strand (light red, inverted) are plotted with respect to TATA box (0 mismatches) (Rhee and Pugh 2012), orientated so that transcription proceeds to the *right*. Filled plots represent no heat shock, compared to unfilled dark traces representing 3 and 6 minutes of heat shock. (*B*) Heat map of TFIIB PIP-seq (permanganate ChIP-seq) tag 5' ends (normalized and shifted), separated into panels with different -1 nucleotides (relative to the sequenced tag 5' end). Note that permanganate/piperidine treatment causes cleavage immediately 3' to "T", with cleavage at other nucleotides representing background cleavage of ChIP'd DNA caused by the piperidine. Data are organized as in Fig. 2. The *bottom* composite plots quantify tag enrichment, based on the composition of the -1 nucleotide, comparing ChIP-exo to PIP-seq. (*C*) Data quantification from heat maps of TFIIB (Sua7) ChIP-exo (green) and PIP-seq (black) from Fig. 7B. Gene classes are as in Figure 3.

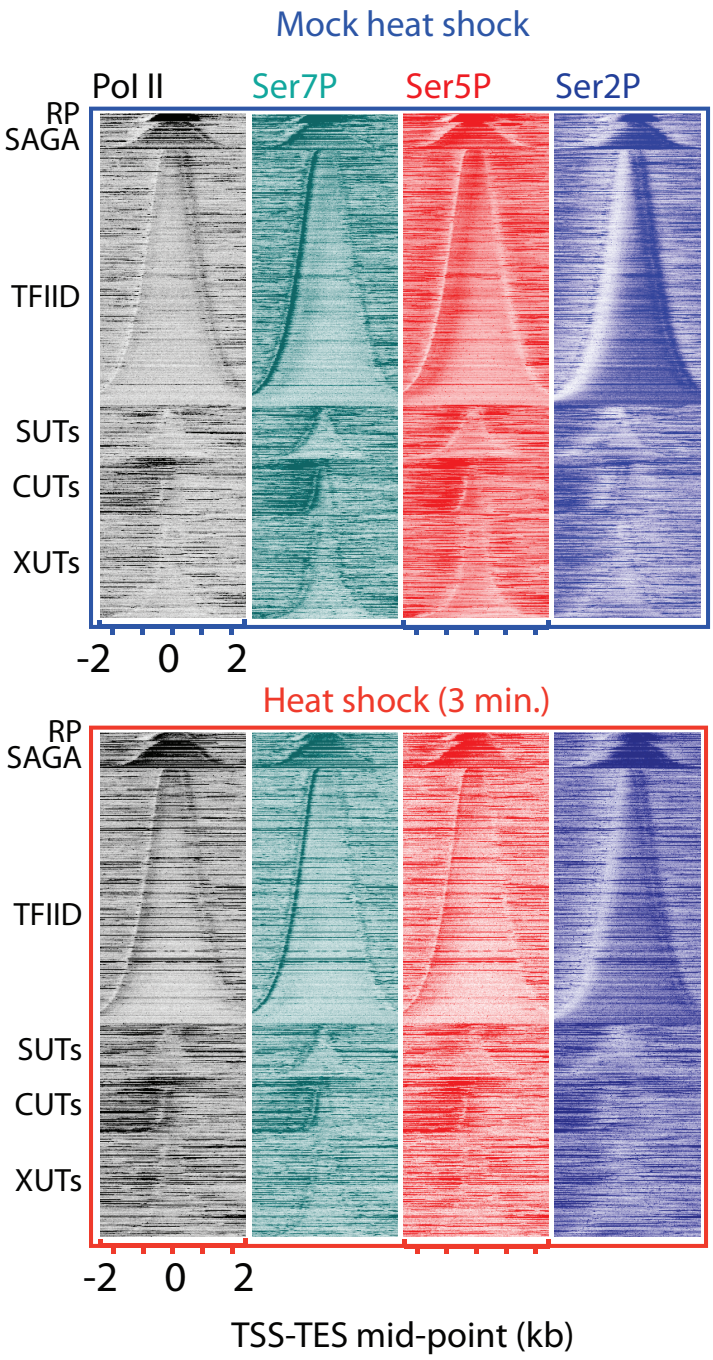

Supplemental Figure S8. CTD phosphorylation at all transcription units before and after heat shock. Data were processed and represented as in Fig. 2: Pol II (black) S7P (teal), S5P (red), and S2P (blue).